

Tracing two-neutron halos in N=20 and 28 isotones: A three-body quest

Jagjit Singh

jagjit.singh@manchester.ac.uk

08.10.2024

.....



Selected Topics in Nuclear and Atomic Physics 2024

Oct 4–8, 2024
Fiera di Primiero (TN),

Europe/Rome timezone



My last Fiera Meeting in 2015- Remembering Prof. Andrea Vitturi



Fiera di Primiero: October 2015



PUNJAB: Birth and Education



PADOVA: 2013-2016 (Ph.D)

800
ANNI



HOKKAIDO: 2016-2019
RCNP OSAKA: 2019-2021



WARSAW: 2022-2022



MANCHESTER: 2022-till date

Rutherford Desk at UoM



Galileo Desk at Padova

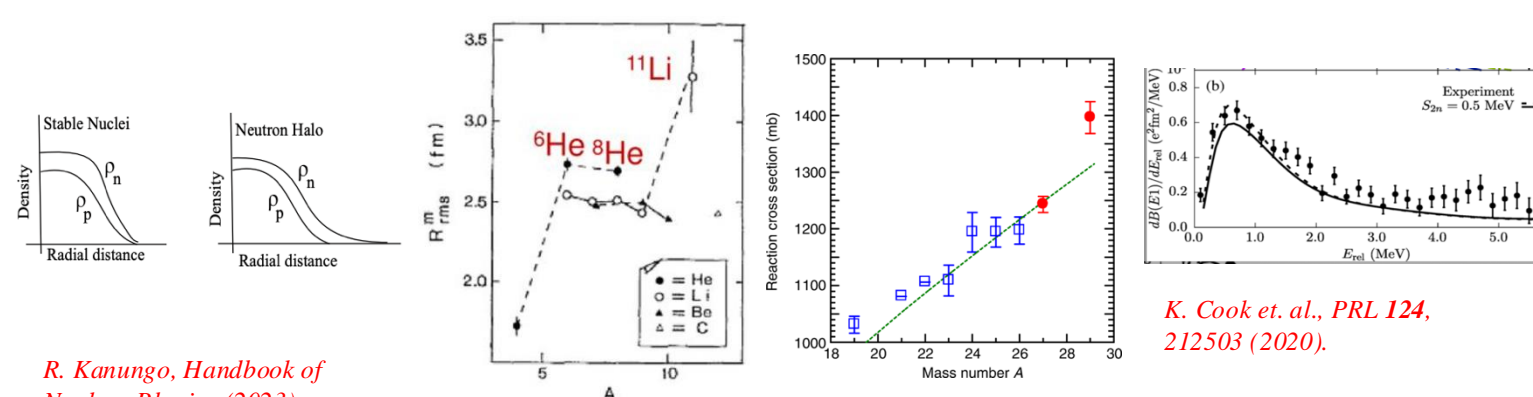
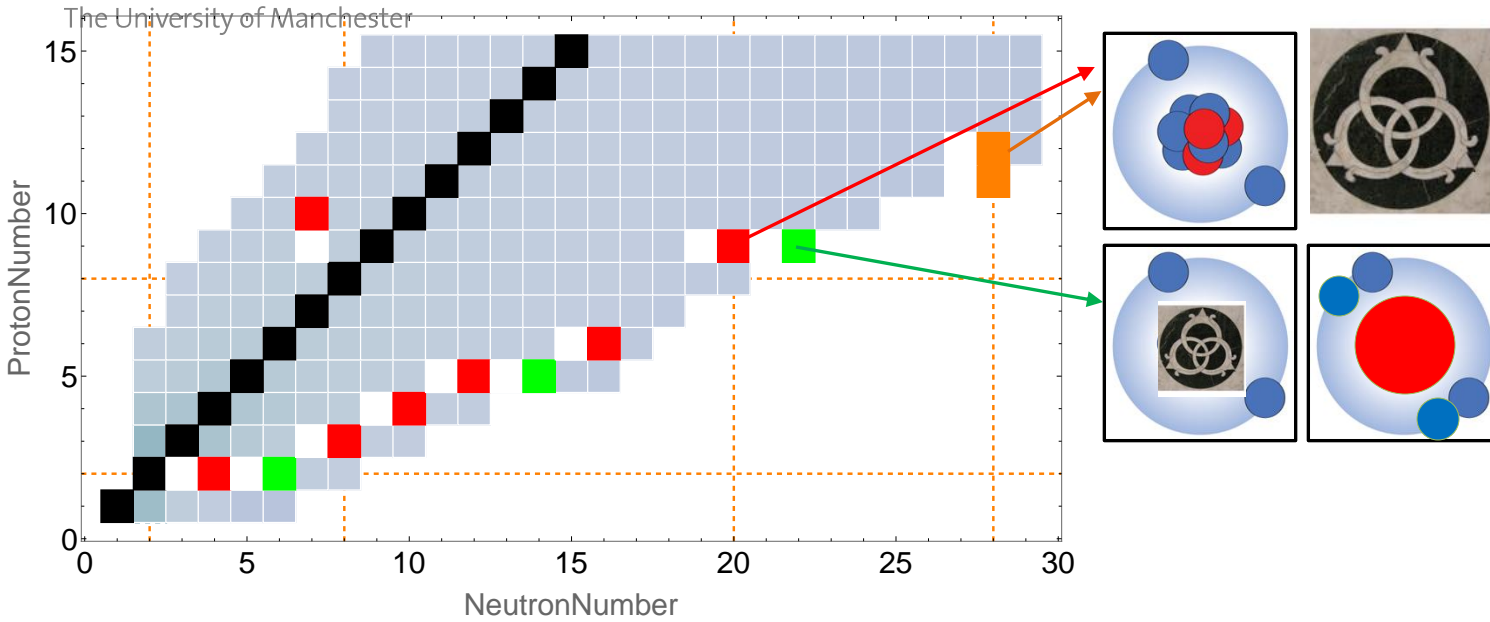


Yukawa Desk at Kyoto



Research Interests: Research and development of few-body approaches for investigating structure and reactions of exotic nuclei (halos/Borromean), Compton scattering, Breakup reactions, Nuclear Data (EXFOR compilation and ENSDF evaluation).

Introduction: Borromean systems



R. Kanungo, *Handbook of Nuclear Physics* (2023).

I. Tanihata et al.,
PRL 55, 2676 (1985).
PLB 160, 380 (1985).

S. Bagchi et al., *PRL*
124, 222504 (2020).

Key features of Borromean nuclei :

- Corresponding subsystems are unbound.
- Low two nucleon separation energies ($s_{2n/p}$).
- Diffuse matter density distribution.
- Abnormally large matter radius.
- Large reaction/interaction cross sections.
- Strong correlations between the valence neutrons are key in binding two-neutron halos.
- Enhanced low-lying $E1$ strength.

M. Zhukov et. al., *Phys. Rep.* 231, 151 (1993).

P. G. Hansen and B. Jonson, *Europhys. Lett.* 4, 409 (1987).

K. Hagino and H. Sagawa, *PRC* 72, 044321 (2005).

M. Matsuo, *PRC* 73, 044309 (2006).

A. Gezerlis, *PRC* 81, 025803 (2010).

Y. Kikuchi et al., *PTEP* 2016, 103D03 (2016).

T. Aumann, *EPJA* 55, 234 (2019).

Theoretically three-body ($\text{core}+n+n$) models describe reasonably well these features in **Borromean nuclei**.

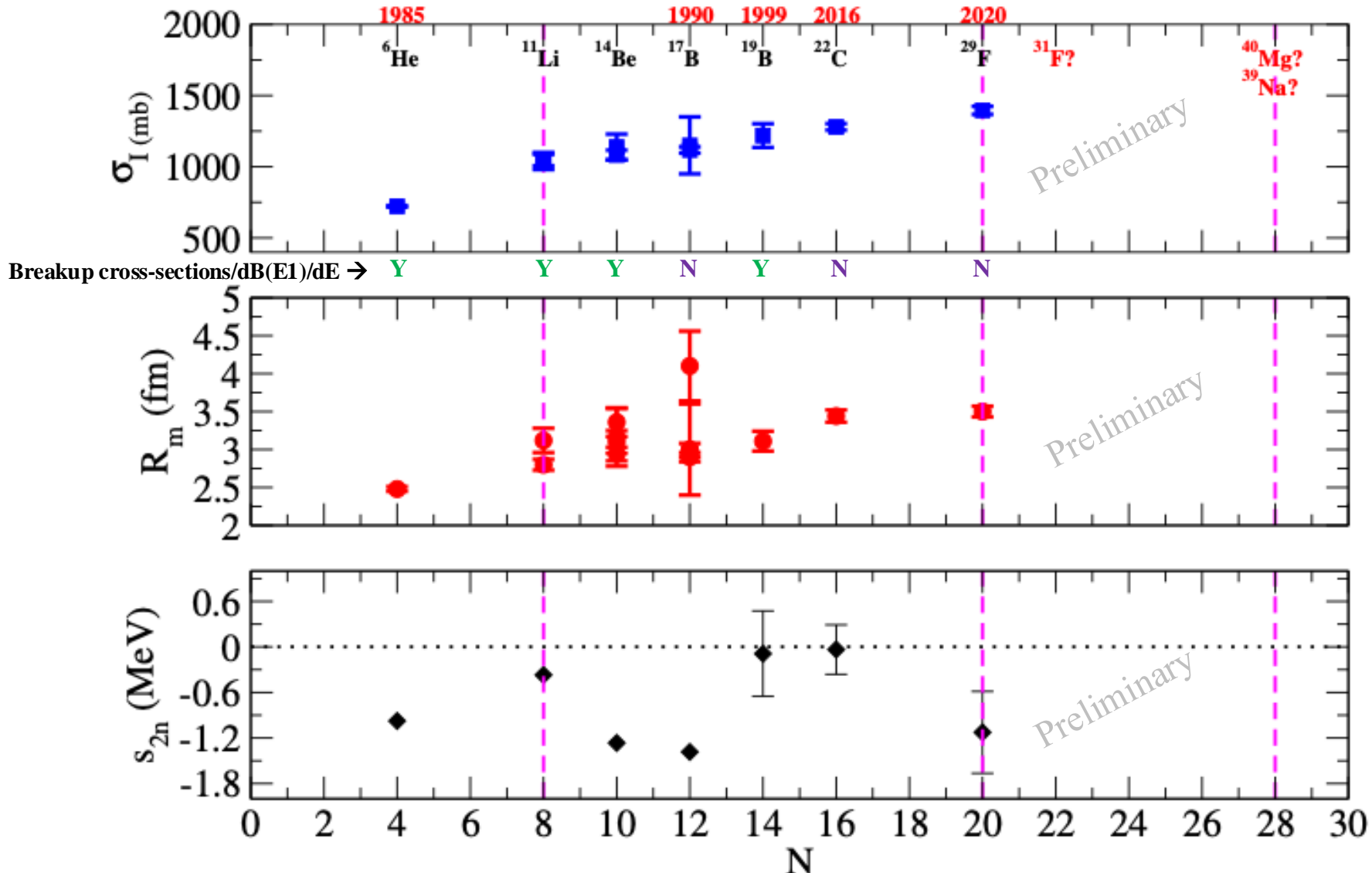
Key inputs for these models are:

- Information on $\text{core}+n$ low-lying spectrum
- Two-neutron separation energy.

JS, *PhD thesis, University of Padova (2016)*.

J. Casal, *Ph.D. thesis, Universidad de Sevilla (2016)*.

Current Status of 2n-halos (Borromean's)



- Tanihata et al., *PRL* **55**, 2676 (1985).
- I. Tanihata et al., in: W.D. Meyers, J.M. Nischke, E.B. Norman (Eds.), *Radioactive Nuclear Beams*, World Scientific, p. 429, (1990).
- T. Suzuki et al., *Nucl. Phys. A* **658**, 313 (1999).
- A. Ozawa et al., *Nuclear Physics A* **693**, 32 (2001).
- Y. Togano et al., *Phys. Lett. B* **761**, 412 (2016).
- S. Bagchi et al., *PRL* **124**, 222504 (2020).
- AME 2021: M. Wang et. al., *CPC* **45** (3) 030003 (2021).
- T. Aumann, et al., *Phys. Rev. C* **59**, 1252 (1999).
- J. Wang, et al., *Phys. Rev. C* **65**, 034306 (2002).
- T. Nakamura, et al., *PRL* **96**, 252502 (2006).
- K. Cook et. al., *PRL* **124**, 212503 (2020).
- Y. Sun et. al., *PLB*, **814**, 136072 (2021).

${}^{31}\text{F?}$:

- N. Michel et. al., *PRC* **101**, 031301(R) (2020).
- H. Masui et. al., *PRC* **101**, 041303(R) (2020).
- GS, JS, et al., *PRC* **105**, 014328 (2022).

${}^{40}\text{Mg}$

- T. Baumann et. al., *Nature* **449**, 1022 (2007).
- H. Crawford et. al., *PRL* **122**, 052501 (2019).

${}^{39}\text{Na}$

- K. Y. Zhang et. al., *PRC* **107** (2023) L041303,

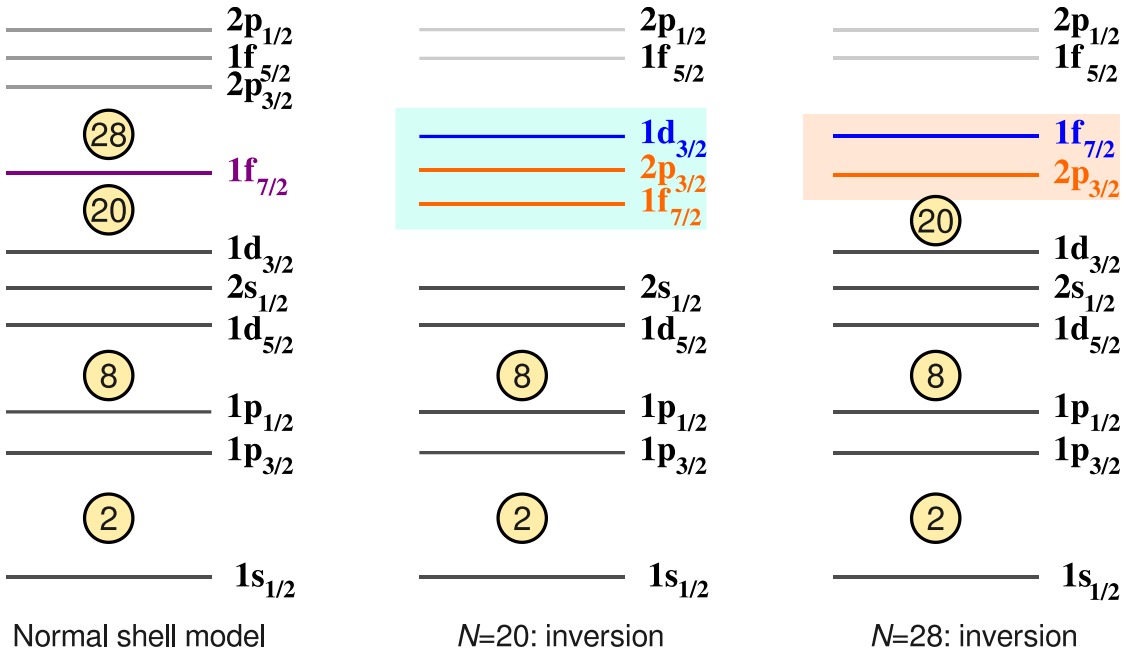
^{33}Si	^{34}Si	^{35}Si	^{36}Si	^{37}Si	^{38}Si	^{39}Si	^{40}Si	^{41}Si	^{42}Si	^{43}Si	^{44}Si	^{45}Si
^{32}Al	^{33}Al	^{34}Al	^{35}Al	^{36}Al	^{37}Al	^{38}Al	^{39}Al	^{40}Al	^{41}Al	^{42}Al	^{43}Al	
^{31}Mg	^{32}Mg	^{33}Mg	^{34}Mg	^{35}Mg	^{36}Mg	^{37}Mg	^{38}Mg	^{39}Mg	^{40}Mg	^{41}Mg		
^{30}Na	^{31}Na	^{32}Na	^{33}Na	^{34}Na	^{35}Na	^{36}Na	^{37}Na	^{38}Na	^{39}Na	^{40}Na		
^{29}Ne	^{30}Ne	^{31}Ne	^{32}Ne	^{33}Ne	^{34}Ne							
^{28}F	^{29}F	^{30}F	^{31}F									

N=28

N=20

- Recent observation of the disappearance of the $N = 20$ shell gap at the low-Z side of the $N = 20$ chain, led to the identification of the ^{29}F system as the heaviest known two-neutron Borromean-halo nucleus. *S. Bagchi et al., PRL 124, 222504 (2020).* *JS, JC et. al., PRC 101, 024310 (2020).* *LF, JC, WH, JS et. al., Comm. Physics 3, 132 (2020).* *JC, JS, et. al., PRC 102, 064227 (2020).*
 - Motivated by this observation, it is interesting to explore the low-Z side of the $N = 28$ shell closure for potential two-neutron Borromean halos in the Na and Mg isotopes.
- A. O. Macchiavelli, et al., Eur. Phys. J. A 58, 66 (2022).*

2n-halo formation on lower Z-side of the magic numbers N=20 and 28



- Inversion occur, when energy gap, associated with filling of shell closures disappears.
- Active shells at $N = 20$ and $N = 28$ shown with coloured blocks. The 1f_{7/2} orbit is bordered by two magic numbers, i.e., 20 and 28.

E. Caurier et. al., Phys. Rev. C 90, 014302 (2014).
O. Sorlin et. al., PPNP 61 (2), 602–673, (2008).
T. Otsuka et. al., Rev. Mod. Phys. 92, 015002 (2020).
JS, J. Casal et al., Physics Letters B 853, 138694 (2024).

Three-Body Structure Model- Hyperspherical framework

Three-body Hamiltonian is given by

$$H = T + \sum_{i=1}^2 V_{core+n_i} + V_{nn} + V_{3b}$$

$$V_{core+n_i} = \left(-V_0 + V_{ls} \vec{l} \cdot \vec{s} \frac{1}{r} \frac{d}{dr} \right) \frac{1}{1 + \exp\left(\frac{r-R}{a}\right)}, \quad V_{3b}(\rho) = v_{3b} e^{-(\rho/\rho_0)^2},$$

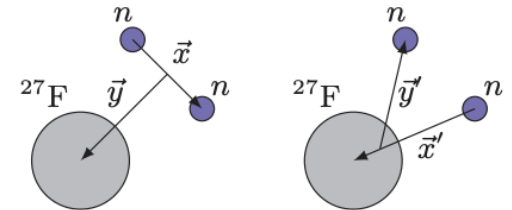


FIG. 1. Jacobi- T (left) and $-Y$ (right) coordinates for the ^{29}F nucleus described as $^{27}\text{F} + n + n$.

nn interaction- Gogny-Pires-Tourreil (GPT) interaction including central, spin-orbit and tensor terms.

[D. Gogny, P. Pires, and R. D. Tourreil, PLB 32, 591 \(1970\).](#)

The three-body force is modelled as a simple Gaussian potential, where $\rho = \sqrt{x^2 + y^2}$, is **hyper-radius** and $\rho_0=6$ fm and the strength v_{3b} is adjusted to recover s_{2n} .

We use the analytical transformed harmonic oscillator (THO) basis.

[J. Casal, M. Rodriguez-Gallardo, and J. M. Arias, Phys. Rev. C 88, 014327 \(2013\).](#)

The diagonalization of the three-body Hamiltonian requires the computation of the corresponding kinetic energy & potential matrix elements. **Spherical inert core approximation is used.**

Reaction cross-section within Glauber model

The reaction cross section for a projectile-target collision integrating the reaction probability with respect to the impact parameter b

$$\sigma_R = \int d\mathbf{b} (1 - |e^{i\chi(\mathbf{b})}|^2),$$

Phase shift function

$$e^{i\chi(\mathbf{b})} = \langle \Phi_0^P \Phi_0^T | \prod_{i=1}^{A_P} \prod_{j=1}^{A_T} [1 - \Gamma_{NN}(s_i^P - s_j^T + \mathbf{b})] | \Phi_0^P \Phi_0^T \rangle$$

Profile function $\Gamma_{NN}(b) = \frac{1 - i\alpha}{4\pi\beta} \sigma_{NN}^{\text{tot}} \exp\left(-\frac{b^2}{2\beta}\right)$

PF describes interaction between projectile and target nucleons is expressed as

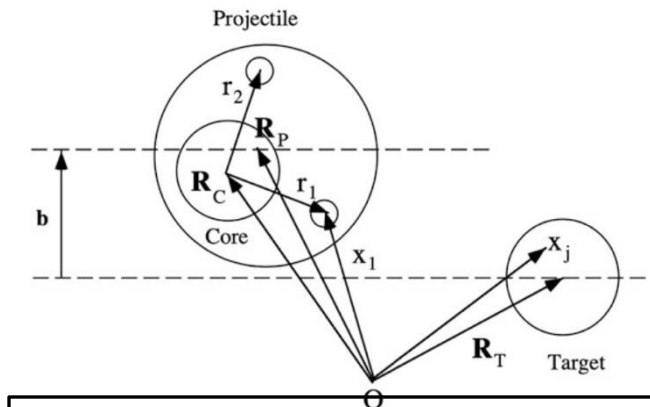
α, β : determined so as to reproduce the NN scattering

B. Abu-Ibrahim et al., PRC 77, 034607 (2008). W. Horiuchi et al., PRC 75, 044607 (2007).

Phase-shift function: Many-body operator

Approximate using a cumulant expansion: Nucleon-Target profile function

→ Input: **Nuclear density and Profile function no adjustable parameters**



- $\mathbf{r}_i = (\mathbf{s}_i, \mathbf{z}_i)$ is the coordinate of the two-halo neutron(s) with index $i = 1, 2$.
- \mathbf{R}_C , \mathbf{R}_p , and \mathbf{R}_T are the position vectors to the COM of the core nucleus, projectile nucleus, and target nucleus, respectively. $\mathbf{x}_i - \mathbf{R}_C = \mathbf{r}_i$.
- \mathbf{s}_i and \mathbf{s}_j are the two-dimensional vectors of the coordinates for the P and T, measured from their COM which lies on a plane perpendicular to the incident momentum of the projectile

^{29}Ne (-1p) on beryllium target : Exploring the low-Z shore of the Island of Inversion at $N = 19$

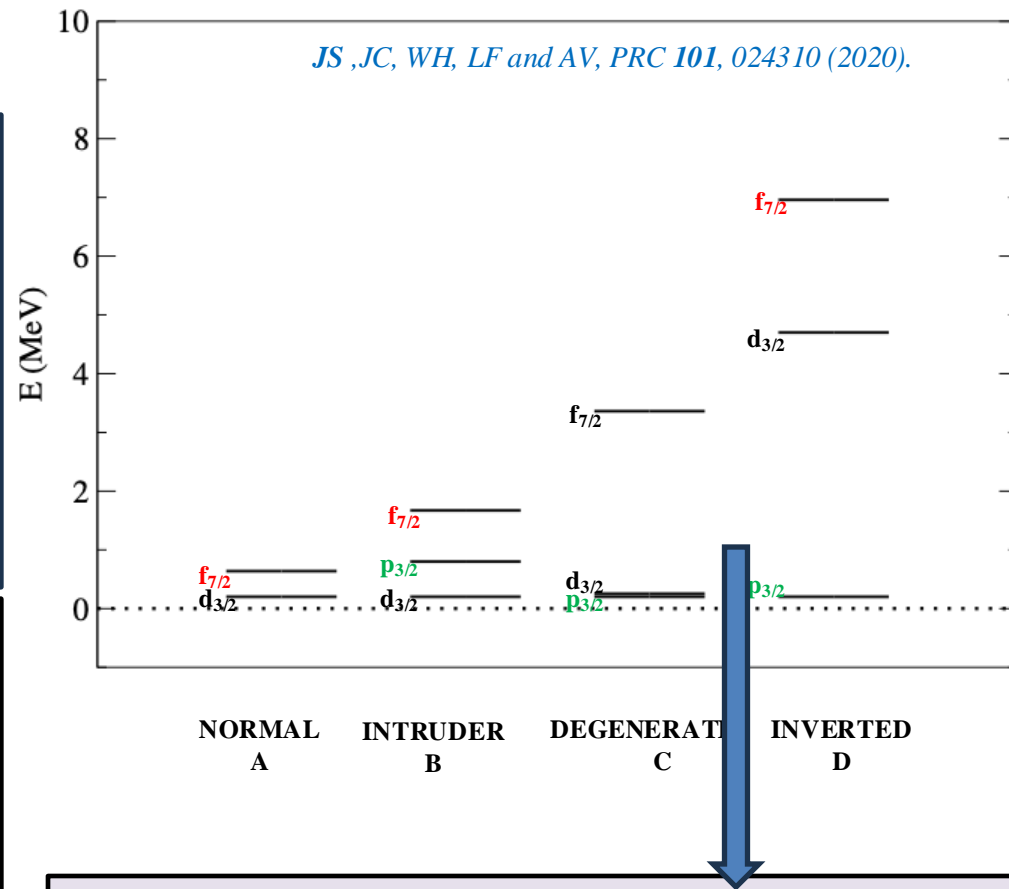
G. Christian et al., PRL 108, 032501 (2012).

Spectroscopy of neutron-unbound $^{27,28}\text{F}$

G. Christian et al., PRC 85, 034327 (2012).

Two resonance model with lower resonance at **220(50) keV [width = 10 keV]** and the upper resonance at **810 keV [width = 100 keV]**

Tale of ^{29}F -I



Recently new data arrived

A. Revel et al., PRL 124, 152502 (2020).

The relative-energy spectra and momentum distributions extracted from high precision nucleon-knockout data

^{29}Ne (-1p) and ^{29}F (-1n) showed

-- ground state resonance of ^{28}F at 0.199(6) MeV ($l=1 \sim 79\%$)

Inversion !!

-- 1st excited state resonance around 0.966 MeV ($l=2 \sim 72\%$)

JS ,JC, WH, LF and AV, PRC 101, 024310 (2020).

Set	S_{2n} (MeV)	$(d_{3/2})^2$	$(f_{7/2})^2$	$(p_{3/2})^2$	R_m (fm)	ΔR (fm)
A	0.400	78.7	8.1	9.0	3.363	0.145
	0.790	80.0	8.3	7.9	3.343	0.125
	1.440	81.3	8.4	6.8	3.323	0.105
	2.090	82.3	8.5	6.0	3.311	0.093
B	0.400	43.2	18.0	30.8	3.420	0.202
	0.790	46.8	19.6	26.2	3.380	0.162
	1.440	50.7	21.1	21.6	3.347	0.129
	2.090	53.4	22.0	18.5	3.329	0.111
C	0.400	30.3	5.6	55.7	3.507	0.289
	0.790	37.3	6.5	48.2	3.434	0.216
	1.440	45.4	7.4	39.8	3.380	0.162
	2.090	51.4	8.0	33.9	3.352	0.134
D	0.400	2.8	1.5	87.6	3.598	0.380
	0.790	3.4	1.7	86.7	3.520	0.302
	1.440	4.2	2.1	85.4	3.459	0.241
	2.090	5.0	2.3	84.2	3.425	0.207

LF, JC, WH, JS and AV, Communication Physics 3, 132 (2020).

JC, JS, LF, WH and AV, PRC 102, 064227 (2020).

Tale of ^{29}F -II

New Experiment confirms ground state resonance of ^{28}F at **0.199(6) MeV (l=1~79%)** and 1st excited state resonance around **0.966 MeV (l=2~72%)**. **Inversion !!**

A. Revel et al., PRL 124, 152502 (2020).

Total reaction Cross section within Glauber Model

The calculated total reaction cross section using the standard Glauber theory are **1370 mb** if we assume $s_{2n} = 1.44 \text{ MeV}$, and **1390 mb** if we take the lower limit ($S_{2n} \approx 1 \text{ MeV}$), which are in good agreement with the observed interaction cross section.

LF, JC, WH, JS and AV, Communication Physics 3, 132 (2020).

JC, JS, et. al., PRC 102, 064627 (2020).

$s_{2n} ({}^{29}\text{F}) = 1.443 (436) \text{ MeV}$ *L. Gaudefroy et al., PRL. 109, 202503 (2012).*
 $= 1.440 (650) \text{ MeV}$ *AME 2017.*

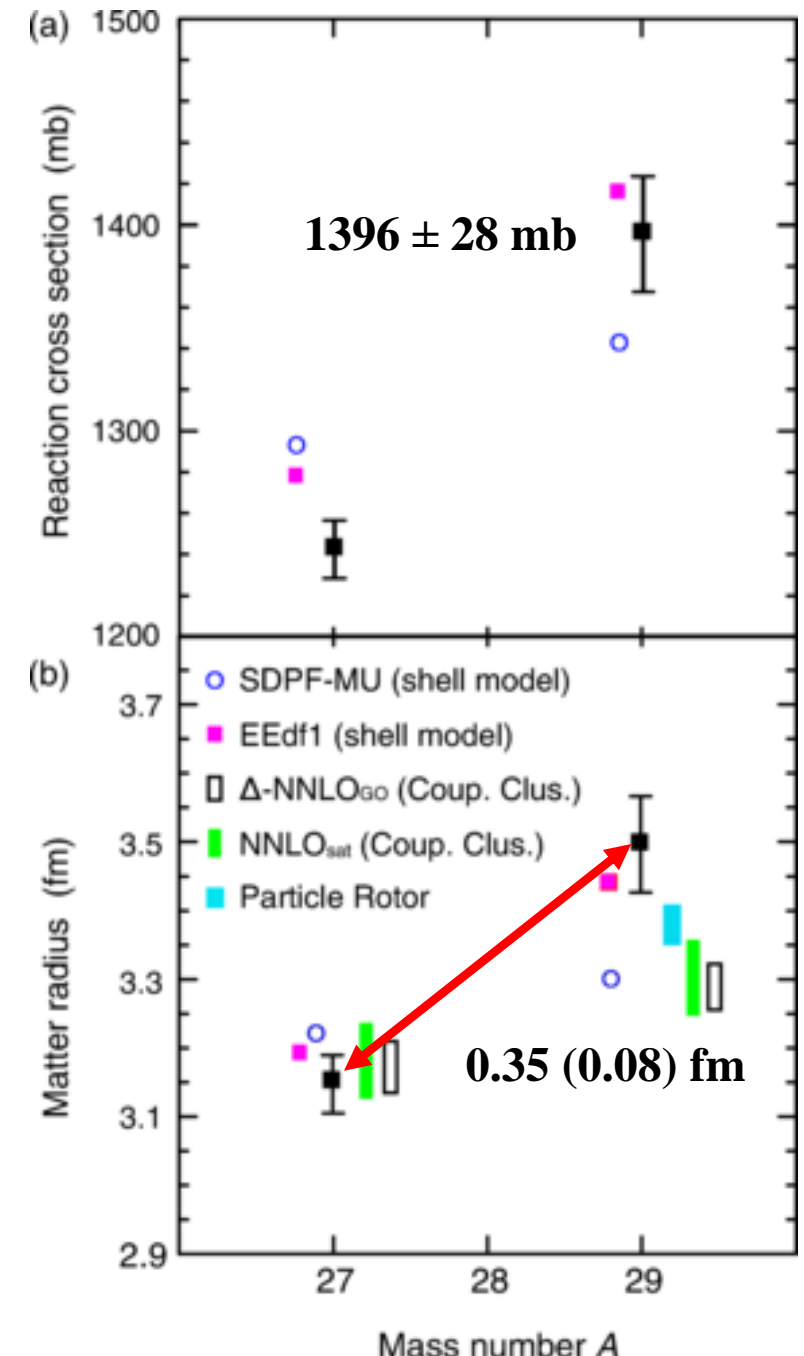
Matter radius of ^{29}F

The relative increase of matter radii with respect to ^{27}F core lies in the range **0.20-0.30 fm** in the different choices of s_{2n} .

JS ,JC, WH, LF and AV, PRC 101, 024310 (2020).

LF, JC, WH, JS and AV, Communication Physics 3, 132 (2020).

JC, JS, LF, WH and AV, PRC 102, 064227 (2020).



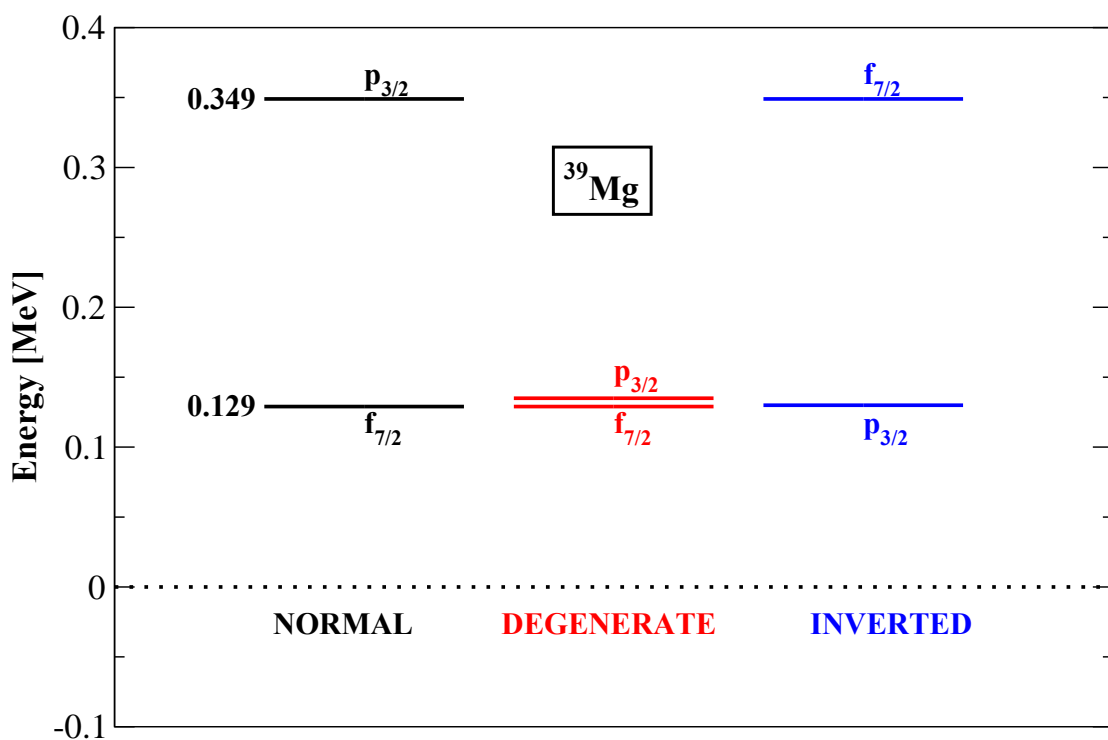
S. Bagchi et al., PRL 124, 222504 (2020).

Two-body (core+n) models for ^{39}Mg and ^{38}Na

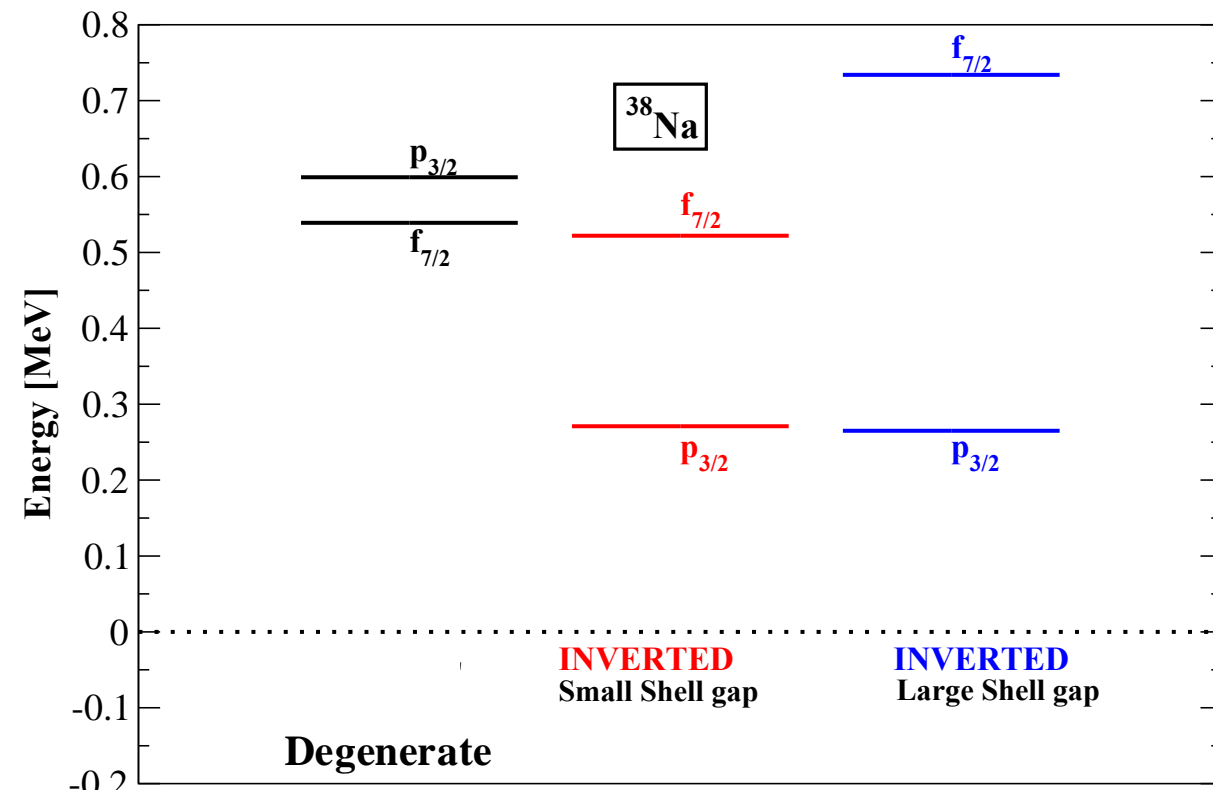
[K. Fossez, et. al., PHYSICAL REVIEW C 94, 054302 \(2016\).](#)

Unbound ground state of ^{39}Mg is predicted to be either a $J^\pi = 7/2^-$ or $3/2^-$ state.

A narrow $J^\pi = 7/2^-$ or $3/2^-$ ground-state candidate exhibits a resonant structure at 129 KeV.



As we do not have either theoretical or experimental predictions and data for ^{38}Na , we use the same **core+n** potential parameters as for ^{39}Mg . The only changes are $R_c=1.25A^{1/3}$ and the spin-orbit strength.



Configuration mixing and matter radii for ^{40}Mg and ^{39}Na

^{40}Mg (s_{2n}) = 0.670 (0.710) MeV

M. Wang, et. al., Chinese Physics C 45 (3), 030003 (2021).

Matter radius of core ^{38}Mg =3.60 fm

S. Watanabe, et. al., PRC 89, 044610 (2014).

^{39}Na (s_{2n}) = unbound

M. Wang, et. al., Chinese Physics C 45 (3), 030003 (2021).

^{39}Na (s_{2n}) = bound (Contradicts AME)

D. S. Ahn et al., PRL 129, 212502 (2022).

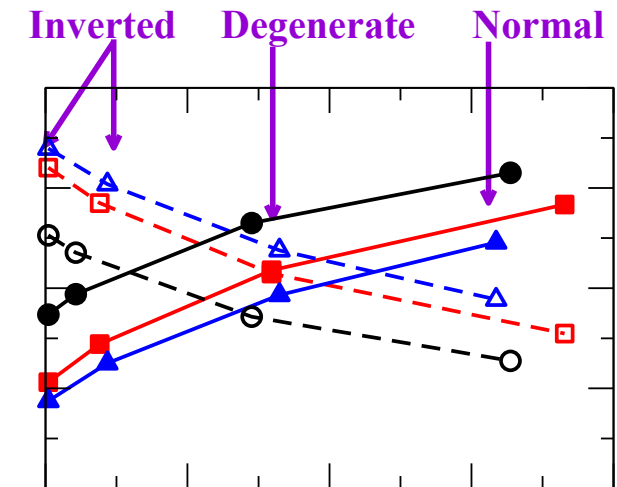
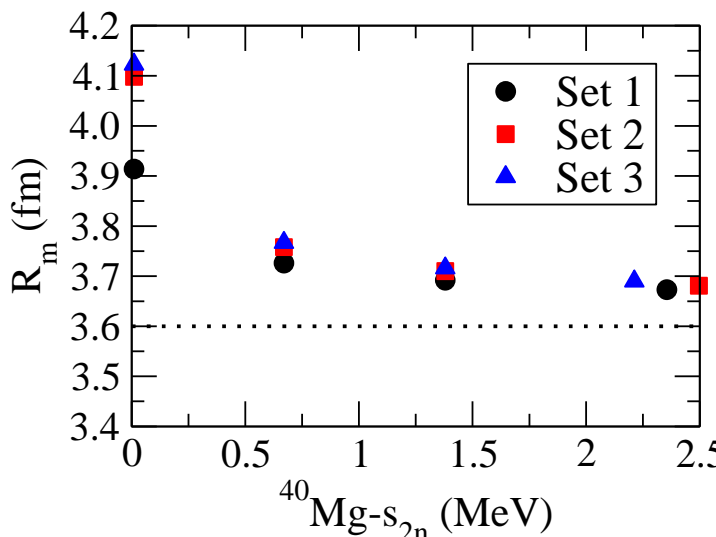
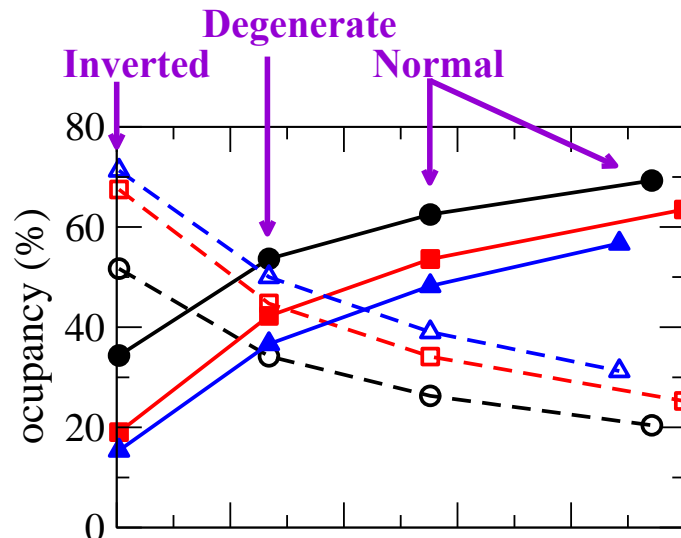
Matter radius of core ^{37}Na =3.64 fm

L. Geng, et. al., NPA 730, 80 (2004).

Our predictions for s_{2n} of ^{39}Na

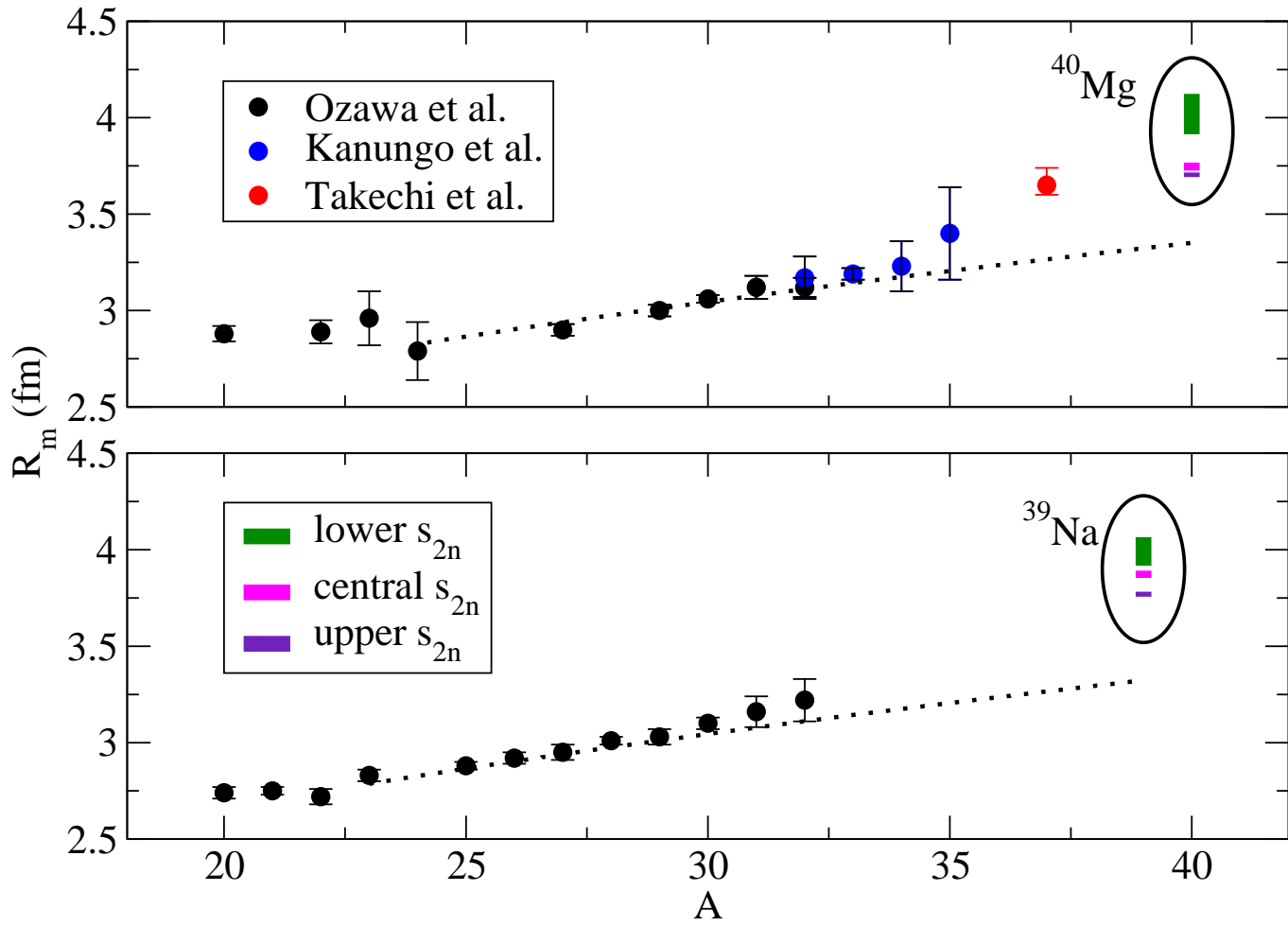
0.010-0.824 (1.828) MeV

The larger change in R_m w.r.t core involves wave function which contains significant $(p_{3/2})^2$ (dotted lines) weight, pointing toward the necessity of intruder configurations to sustain halo formation. $(f_{7/2})^2$ (solid lines)



Matter radii for ^{40}Mg and ^{39}Na

- Dotted black lines in the figure correspond to the weighted fit of the experimental data points with the standard $R_0 A^{1/3}$ formula.
- The radii of ^{40}Mg and ^{39}Na are higher than the standard fitted value.
- This observation implies a likely two-neutron halo structure in the ground state of ^{40}Mg and ^{39}Na , and the corresponding melting of the traditional $N = 28$ shell gap is due to the intrusion of the $p_{3/2}$ orbital.



- Ozawa *et al.*, Nuclear Physics A **691** (3), 599 (2001).
- Kanungo *et al.*, Phys. Rev. C **83**, 021302 (2011).
- Takechi *et al.*, Phys. Rev. C **90**, 061305(R) (2014).
- JS, J. Casal *et al.*, Physics Letters B **853**, 138694 (2024).

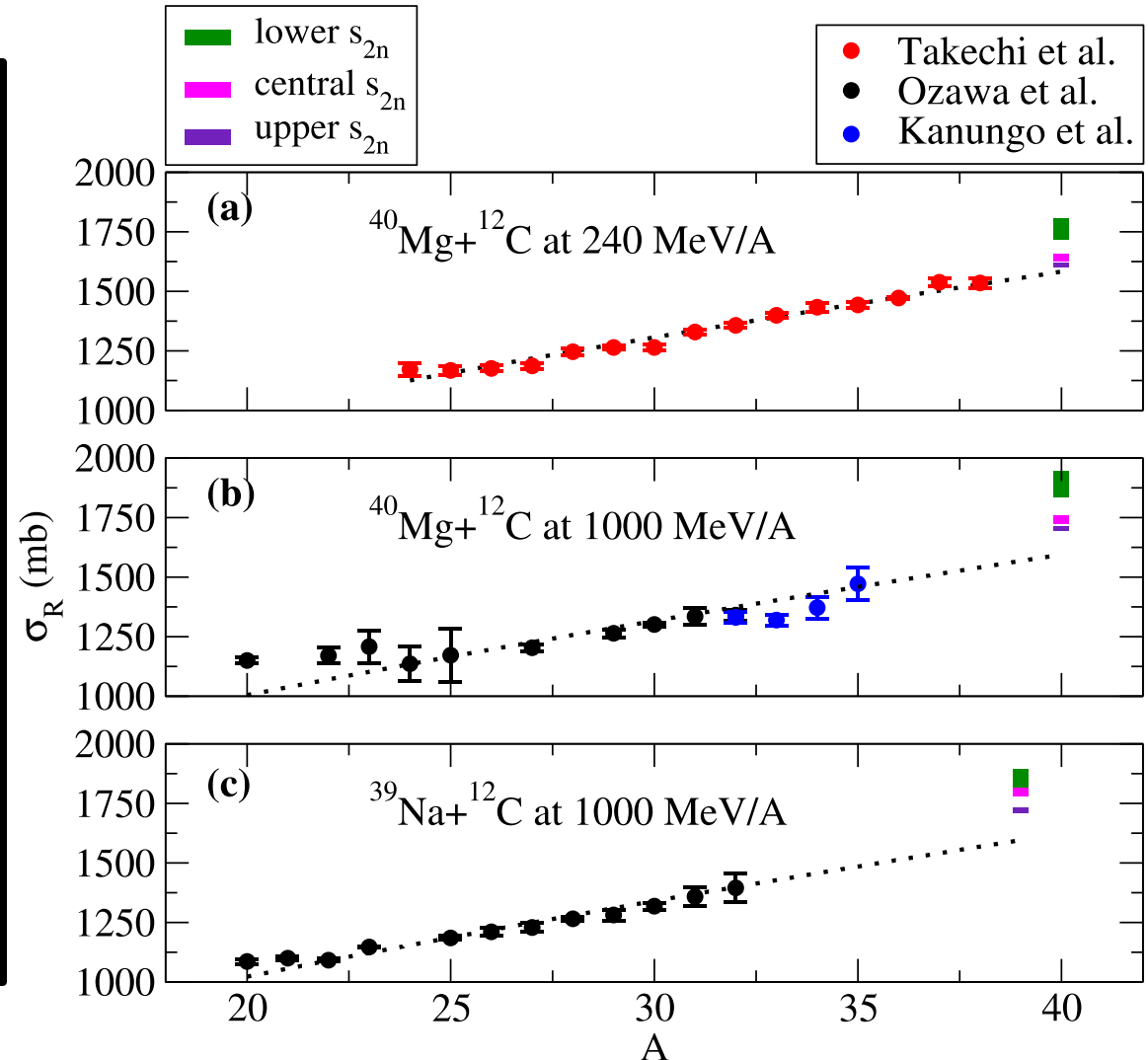
Reaction cross-sections for ^{40}Mg and ^{39}Na : within Glauber reaction theory

- Experimentally, a very obvious way to determine whether a nucleus is a halo nucleus, is to look for an enhanced reaction cross section. Thus, we examine the total reaction cross section by employing the conventional Glauber theory. [B. Abu-Ibrahim et al., PRC 77, 034607 \(2008\)](#). [W. Horiuchi et al., PRC 75, 044607 \(2007\)](#).

- Using this prescription, we predict the σ_R for ^{40}Mg and ^{39}Na at different incident energies. The predicted values of σ_R for ^{40}Mg and ^{39}Na show significant enhancement with respect to the observed σ_R in the lower-A isotopes for both choices of energy.

Thus, our results provide a clear signal of the 2n-halo structure formation in ^{40}Mg and ^{39}Na and hence melting of the N = 28 shell closure.

- [Ozawa et al., Nuclear Physics A 691 \(3\), 599 \(2001\)](#).
- [Kanungo et al., Phys. Rev. C 83, 021302 \(2011\)](#).
- [Takechi et al., Phys. Rev. C 90, 061305\(R\) \(2014\)](#).
- [JS, J. Casal et al., Physics Letters B 853, 138694 \(2024\)](#).

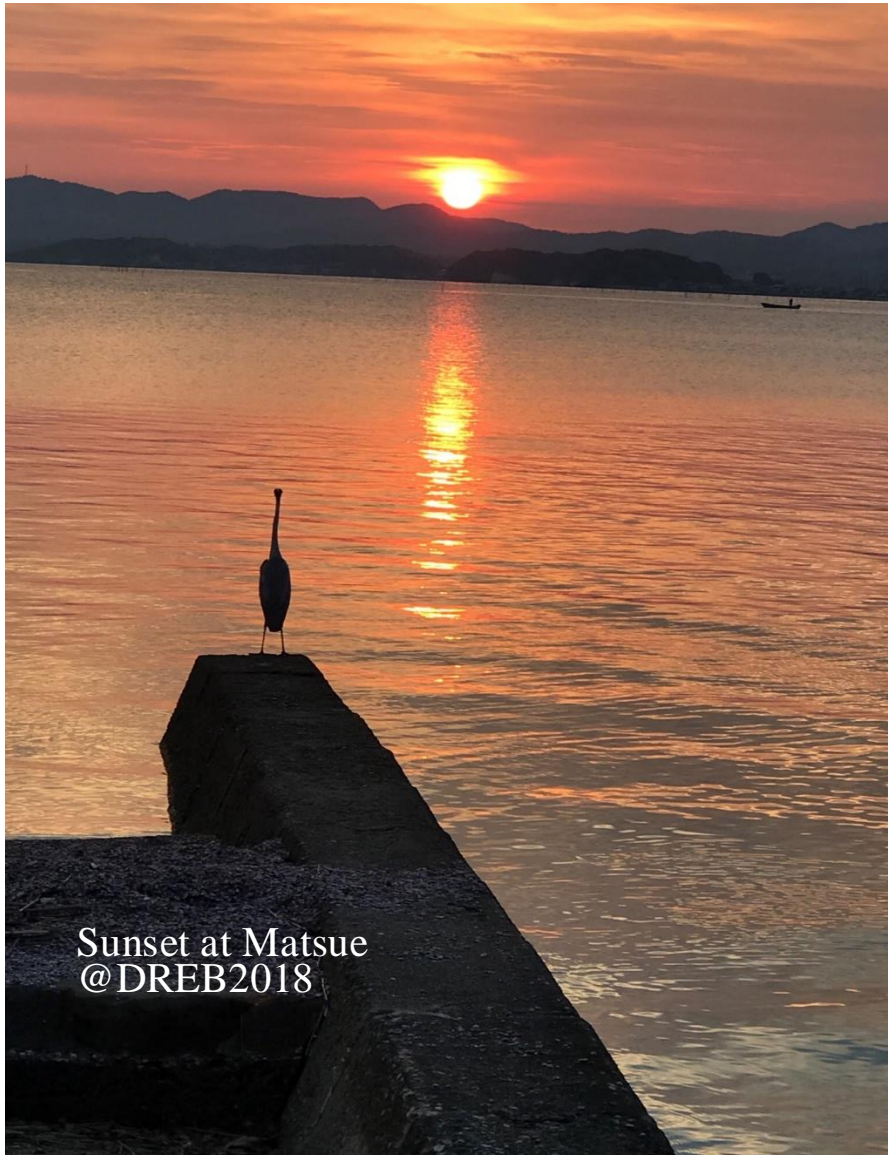


Summary:

- We started with studying melting of N=20 (*JS, JC, WH, LF, and AV, PRC 101, 024310 (2020)*) for ^{29}F . Our results/predictions got boost with new measurements (*S. Bagchi et al., PRL 124, 222504 (2020) and A. Revel et al., PRL 124, 152502 (2020)*). We updated our calculations with precise calculations along with detailed analysis of electric-dipole response and reaction calculations (*LF, JC, WH, JS, and AV, Commun. Phys. 3, 132 (2020) and JC, JS, LF, WH, and AV, PRC 102, 064627 (2020)*).
- Motivated by melting N=20 ends up in formation of Borromean in ^{29}F , by using same prescription we reported first three body results for ^{39}Na and ^{40}Mg lying on low-Z side of N=28. (*JS, J. Casal et al., Physics Letters B 853, 138694 (2024)*).
- Our results calls for new precise mass measurements for s_{2n} of three-body systems and the low-lying continuum spectrum of two-body subsystems to better constrain the theoretical models.
- The disappearance of the conventional N=28 shell gap and emergence of the halo leads to significant occupancy of intruder $p_{3/2}$ orbit in the ground state of ^{39}Na and ^{40}Mg . Nevertheless, it is imperative to verify this conclusion through experimental measurements of interaction cross sections and tranfer or knock out data to probe partial-wave content.

Future Perspectives:

- It is interesting to see how our predictions are affected with inclusion of core deformation effects.
H. H. Li et al., PHYSICAL REVIEW C 109, L061304 (2024)
- Calculation of electric dipole (E1) response for these systems.



Thanks for kind attention.

Acknowledgements:

- J. Casal (Seville)
- W. Horiuchi (OMU, Osaka)
- N. R. Walet (Manchester)
- W. Satula (Warsaw)
- L. Fortunato (Padova)
- A. Vitturi (Padova)